Article:

Si, Jikai, Yan, Zuoguang, Nie, Rui et al. (3 more authors) (2022) Multi-objective optimization of a tubular permanent magnet linear generator with 120° phase belt toroidal windings using response surface method and genetic algorithm. IET Renewable Power Generation. pp. 352-361. ISSN 1752-1424

https://doi.org/10.1049/rpg2.12328

Received: 5 June 2021 | Revised: 30 July 2021 | Accepted: 29 October 2021

DOI: 10.1049/rpg2.12328

IET Renewable Power Generation

ORIGINAL RESEARCH PAPER

Multi-objective optimization of a tubular permanent magnet linear generator with 120° phase belt toroidal windings using response surface method and genetic algorithm

Jikai Si[1] | **Zuoguang Yan**[1] | **Rui Nie**[1] | **Zhongwen Li**[1] | **Yihua Hu**[2] | **Yingsheng Li**[3]

[1] School of Electrical Engineering, Zhengzhou University, Zhengzhou, China

[2] Department of Electronic Engineering, University of York, York, UK

[3] Technical Department, Zhengzhou Runhua Intelligent Equipment Co., Ltd., Zhengzhou, China

Correspondence
Rui Nie, School of Electrical Engineering, Zhengzhou University, Zhengzhou 450001, China.
Email: nierui@zzu.edu.cn

Funding information
Natural Science Foundation of China, Grant/Award Number: 51777060; Collaborative Innovation in Zhengzhou, Grant/Award Number: 20XTZX12023; China Postdoctoral Science Foundation, Grant/Award Number: 2020M682342

Abstract
In terms of the characteristics of multi-objective and interactions among optimization objectives of the tubular permanent magnet linear generator with 120° phase belt toroidal winding (120°-TPMLG), a multi-objective optimization method is proposed to improve the generators performances, which is based on the combination of response surface method and the genetic algorithm. First, the sensitivity analysis of different structural parameters on the performances of the 120°-TPMLG is conducted to pick out the sensitive structural parameters. Then develop those sensitive parameters as optimization variables to establish the response surface equation of the generator performances including output power (P), detent force (F), and the efficiency (η). Subsequently, based on the surface equation, the genetic algorithm (GA) fitness function is proposed to conducted the global optimization and the optimization results are finally obtained. To verify the effectiveness of the proposed optimization method, the performances of the optimal 120°-TPMLG are analysed and compared with the initial one. The results show that the performances including the detent force and power density of the 120°-TPMLG are greatly improved, which prove that the proposed multi-objective optimization method is effective for the 120°-TPMLG.

1 | INTRODUCTION

LINEAR generator can directly convert wave energy into electrical energy without using intermediate transmission device, so it is widely used in the direct-drive wave energy converter (DD-WEC) systems. Presently, the major linear generator used for the DD-WEC systems are the tubular permanent magnet linear generators (TPMLGs), which inherits the merits of high winding utilization rate and high efficiency [1, 2]. Unfortunately, common TPMLGs used in DD-WEC system have the problem of low power density due to their low operation speed [3, 4]. To alleviate this problem, a TPMLG with 120° phase belt toroidal windings (120°-TPMLG) is proposed. Its analysis results show that the 120°-TPMLG has the advantages that high-power density and high-efficiency [5]. However, the 120°-TPMLG possess multiple structural parameters, and the interaction or even conflict among these structural parameters would have strong impact on generator performances in the optimization process. Consequently, it is full of challenges to design and optimize a feasible 120°-TPMLG, where the generator performances can not only be comparable and competitive with those of the traditional toroidal windings TPMLG (T-TPMLG), but the performances can also realize the advantage of high-power density.

In the process of the generator optimization, due to the same variable may have various sensitivity degrees on the generator performances, the design conflicts always exist among different generator performances [6, 7]. It will bring about the computation complexity and design randomicity on the 120°-TPMLG to large extent. To solve the problem, the comprehensive sensitivity analysis methods have been successfully used to generator optimization process, which can pick out the sensitive structural parameters and realize the fast optimization of those parameters by effectively evaluating the sensitivity of the multiple structural parameters on the generator performances [8, 9]. In [10], the sensitivity analysis method is used to effectively evaluate the sensitivity of the structural parameters and select the sensitive structural parameters in the optimization process of the V-shape flux-modulated permanent-magnet motor. And then the surface response method (RS method) is adopted to optimize those sensitive parameters, where the analytical model between the design objectives and design parameters can be developed to realize the fast search of the best parameter combination. Nevertheless, only two related design parameters can be optimized at the same time. When several structural parameters are selected to be optimized, it is difficult to consider the interaction and mutual conflict among all the selected optimization parameters simultaneously [11]. Therefore, how to optimize multiple design parameters at the same time, as well as effectively realize the optimal designs, are becoming a hot issue and new challenge in the field of motor optimization.

With the fast development of the numerical analysis method, the aforementioned optimization problem can be solved by means of the intelligent optimization algorithms, such as genetic algorithm, particle swarm optimization algorithm, and difference evolution algorithm [12–14]. In [15], Gao Jian adopted the genetic algorithm to optimize the surface-mounted permanent magnet synchronous motor, where multiple design parameters can be concurrently optimized to obtain the best combination of parameters. In [16], Jin Hwan Lee proposed a modified particle swarm optimization algorithm to optimize the permanent magnet synchronous machine, where the motor performances can be effectively improved in the case of more design variables. However, the aforementioned two optimization method have the demerits of time-consuming and spoor-efficiency due to multiple design variables. In [17], Xiaoyong Zhu pick out the sensitive parameters of the double-rotor flux-switching permanent magnet machine (DFPM) using the sensitivity analysis method, and then adopted the genetic algorithm to optimize those parameters, which greatly improve the motor optimization efficiency and realize design objectives of high-toque capability, low-torque ripple, and low-magnetic coupling between the inner and outer motors. However, the establishment and computer analysis of the genetic algorithm fitness function are very complicated and time consuming [18]. To address those problem, a new multi-objective optimization method for the 120°-TPMLG is proposed, where the sensitivity analysis method, RS method, and the genetic algorithm are co-applied to conduct the generator optimization. This method can not only decrease the computation complexity and save computational time, but also establish the genetic algorithm fitness function quickly and accurately. Moreover, it can optimize multiple design parameters at the same time.

The main purpose of this paper is to propose a multilevel optimization design method to improve the generator performances including the power density, efficiency, and detent force. The remainder of this paper is organized as follows. First, the structure of the 120°-TPMLG is introduced in Section 2. In Section 3, the sensitivities of the key structural parameters on the optimization objectives are evaluated quantitatively.

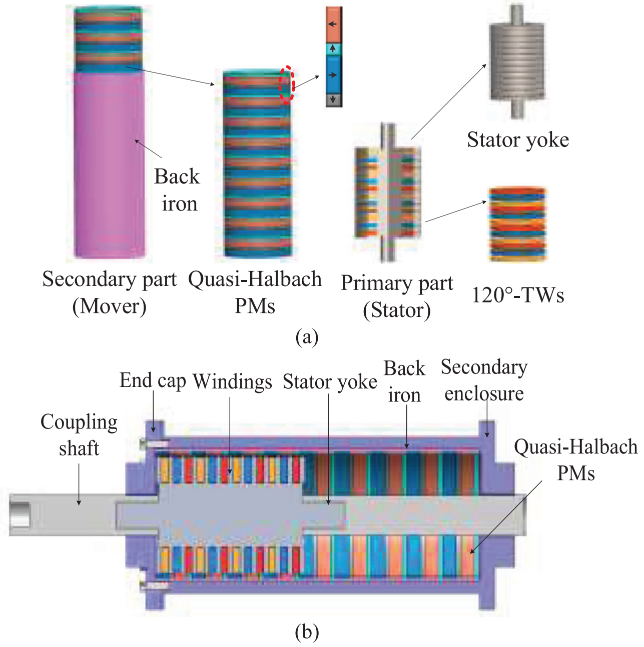

FIGURE 1 The structure of the 120°-TPMLG. (a) Components view of the 120°-TPMLG. (b) Section views of the 120°-TPMLG

Based on the result of sensitivity analysis, four sensitive structural parameters are selected as the optimization variables. In Section 4, the RS method and the genetic algorithm are co-applied to conduct the multi-objective optimization for the 120°-TPMLG. And then, the optimal parameter combination is obtained. In Section 5, the performances of the optimal 120°-TPMLG are analyzed as well compared with the initial one. Finally, the conclusion is drawn in Section 6.

2 | OPTIMIZATION VARIABLE AND OPTIMIZATION OBJECTIVE

2.1 | Structure of the 120°-TPMLG

The 120°-TPMLG is proposed to improve the power density for DD-WEC system. Its structure is depicted in Figure 1.

As shown in Figure 1, the structure of the 120°-TPMLG consists of a primary part (stator) and a secondary part (mover). The primary part, which includes a stator yoke and 120° phase belt toroidal windings (120°-TWs), is fixed. The secondary part, which is made up of permanent magnets (PMs) with quasi-Halbach magnetization and back iron, is connected to the buoy. As the secondary part moves vertically along with the buoy, the magnetic flux generated by the PMs passes the 120° -TWs, and the induction electromotive force is obtained.

To illustrate the structural characteristics of the 120°-TPMLG, the windings configuration of the generator is described and shown in Figure 2. The symbols A, B, C represent the incoming line ends of the windings, and the symbols X, Y, Z represent the outgoing line ends of the windings.

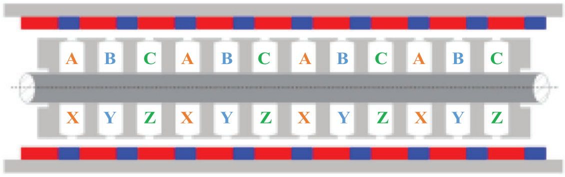

FIGURE 2 Windings configuration of the 120°-TPMLG

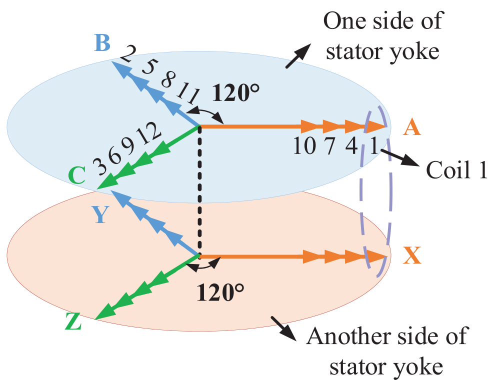

FIGURE 3 Vector diagram of synthetic EMF of the 120°-TPMLG

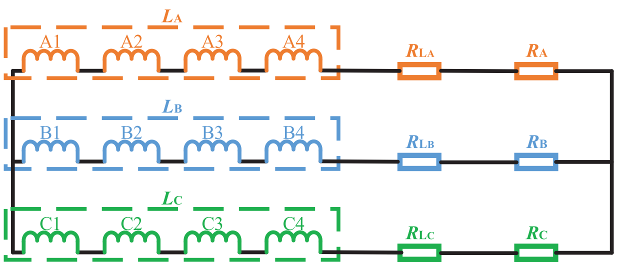

FIGURE 4 The equivalent circuit diagram of the 120°-TPMLG

As shown in Figure 2, the stator yoke of 120°-TPMLG is provided with 12 annular slots along the axial direction, and each slot is embedded with an independent single-layer toroidal winding, which increases the heat dissipation area and improves the thermal performance. Besides, the incoming line ends of the windings of the 120°-TPMLG is not only located on the same side of the stator yoke, but also have the same orientation, which will lead a high winding coefficient and improve the no-load EMF.

To further illustrate the merits of the winding configuration, the vector diagram of synthetic electromotive force and the equivalent circuit diagram of the 120°-TPMLG are described and shown in Figures 3 and 4, respectively. The symbols R_{LA}, R_{LB}, and R_{LC} represent the inner resistance of the three-phase windings, and the symbols R_A, R_B, and R_C represent the resistance of the three-phase loads.

According to the Figures 3 and 4, it can be observed that the synthetic EMF of phase A, B, and C are all on the one side of the stator yoke, and synthetic EMF of phase X, Y, and Z are all on the other side of the stator yoke due to the special layouts of the 120°-TWs. It should be noted that there has no space vector misalignment of coil-EMF, which can effectively increase the EMF and further improve the power density.

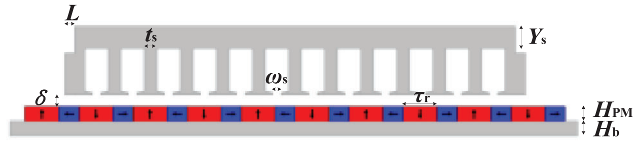

FIGURE 5 Geometric parameters of the 120°-TPMLG

TABLE 1 Candidate variables and their variation ranges

CANDIDATE VARIABLES	INITIAL VALUE	Variation range
H_{PM}/mm	3.5	3.5~4.5
τ_r/mm	21.3	19.6~23
H_b/mm	9.5	9~11
Y_s/mm	12	11~13
δ/mm	4	3.5~4.5
t_s/mm	11	10~12
ω_s/mm	3.7	2.7~4.7
L/mm	5.8	3.8~7.8

2.2 | Optimization variables

The geometric parameters of the 120°-TPMLG are shown in Figure 5.

According to the existing design experience of the conventional TPMLGs, eight key structure parameters are selected to be the candidate variables for optimization, which are PM thickness (H_{PM}), PM length for r direction (τ_r), back-iron thickness (H_b), stator yoke thickness (Y_s), air gap width (δ), stator tooth width (t_s), slot opening width (ω_s), auxiliary tooth width (L), respectively [19]. The initial value and their reasonable variation ranges of those parameters are listed in the Table 1.

2.3 | Optimization objectives

Considering the operation condition of the low direct-drive speed, the output power and the efficiency of the 120°-TPMLG need to be maintained at a desirable degree. Hence, the output power and the efficiency are considered as the optimization objectives. In addition, similar to other linear generators, the 120°-TPMLG always suffers from large detent force, which may inevitably lead to the mechanical vibration, acoustic noise, and even cause operating failures, especially in low-speed and direct-drive applications. Thus, the low detent force is one of the important optimization objectives in the generator optimization process. Therefore, the output power, the efficiency, and the detent force are selected to be the optimization objectives in this paper.

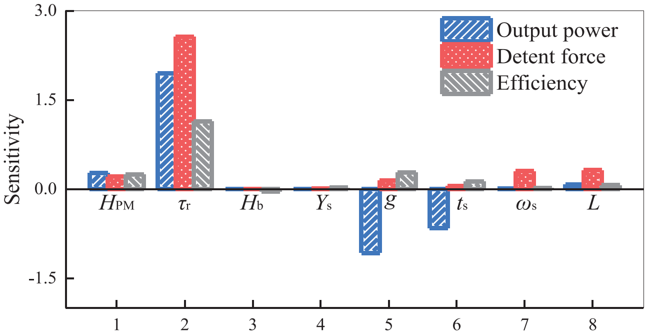

FIGURE 6 Sensitivity indices of the optimization variables to the three optimization objectives

TABLE 2 Sensitive values of design variables

Candidate variables	Optimization objectives $S_P(x_i)$ $\lambda_P = 0.4$	$S_F(x_i)$ $\lambda_P = 0.4$	$S_\eta(x_i)$ $\lambda_P = 0.2$	Sensitivity (S_{com})
H_{PM}	0.2748	0.2090	0.2477	0.2431
τ_r	1.9490	2.5608	1.1420	2.0323
H_b	-0.0009	0.0024	-0.0369	0.0087
Y_s	-0.0001	0.0147	0.0240	0.0107
δ	-1.0727	0.1460	0.2812	0.5437
t_s	-0.6559	0.0521	0.1291	0.3090
ω_s	0.0084	0.3016	0.0225	0.1285
L	0.0794	0.3193	0.0661	0.1727

3 | COMPREHENSIVE SENSITIVITY ANALYSIS

To explicitly reflect the influence of each optimization variable on the optimization objectives, the sensitivity index is introduced based on sensitivity analysis. The corresponding sensitivity index $S(x_i)$ can be given by [20]:

$$S(x_i) = \frac{V\left(E\left(f(x_i)/x_i\right)\right)}{V\left(f(x_i)\right)} \tag{1}$$

where $f(x_i)$ is the optimization objective. $E(f(x_i)/x_i)$ is the average value of $f(x_i)$ when x_i is constant, and $V(E(f(x_i)/x_i))$ is the variance of $E(f(x_i)/x_i)$.

Based on the Equation (1), the sensitivity of optimization variables to the three optimization objectives are calculated and shown in Figure 6.

From the Figure 6, as one can see that the same variable may have different sensitive values on various objectives, and thus leading to the difficulty in the evaluation and selection of sensitive optimization variables. To address the problem, a comprehensive sensitivity S_{com} is introduced and defined as follows:

$$S_{com} = \lambda_P|S_P(x_i)| + \lambda_F|S_F(x_i)| + \lambda_\eta|S_\eta(x_i)\% \tag{2}$$

where the $S_p(x_i)$ is the sensitivity of the output power, $S_F(x_i)$ is the sensitivity of the detent force, $S_\eta(x_i)$ is the sensitivity of the efficiency. λ_P, λ_F, and λ_η are the weight coefficients of the output power, the detent force, and the efficiency, respectively. Considering the application background of the 120°-TPMLG, the power density and the detent force are more important than the efficiency to satisfy the requirements. Consequently, λ_P and λ_F are set as 0.4, which are higher than the weight coefficients of the efficiency ($\lambda_\eta = 0.2$).

The comprehensive sensitivity results are obtained and listed in Table 2.

To clearly evaluate the sensitive degrees of the structural parameters on the performances of the 120°-TPMLG, the structural parameters whose sensitive values higher 0.2 are defined the sensitive structural parameters [21]. Based on the comprehensive sensitivity analysis results in Table 2, it can be observed that the H_{PM}, τ_r, g, and t_s are the sensitive structural parameters. Consequently, the four structure parameters are selected to be the optimization variables.

4 | MULTI-OBJECTIVE OPTIMIZATION

4.1 | Establishment of the objective function

The RS method, as a statistical tool, can be used to build an analytical model by finding the relationship between the design variables and response through statistical fitting method based on the observed data from system [22]. The response can be obtained from real experiments or computer simulation. To build the analytical model between the optimization objectives and the optimization variables, this method is adopted in this paper and the finite element analysis (FEA) is used as numerical experiments to provide the response. And the optimization objectives including the output power, the efficiency, and the detent force are the responses, which are changed by the optimization variables variation.

To find a suitable approximation for the true relationship between optimization objectives and the set of independent optimization variables. Usually, a low-order polynomial of the independent variables is employed [23]. Thereby a first or second-order model is used. To predict an accurate curvature response, the second order polynomial is chosen in this paper, as follows:

$$f(x) = \beta_0 + \sum_{i=1}^{2}\beta_i x_i + \sum_{i=1}^{2}\beta_{ii}x_i^2 + \sum_{i=1,i<j}^{2}\beta_{ij}x_i x_j + \varepsilon \tag{3}$$

where β is the coefficient to be determined, ε is the fitting error, x_i is the optimization variable.

Among the numerous approaches available for construction of a second order model, the central composite design (CCD) is the most popular and efficient one, which is used to build the response surface model in this paper [24]. The optimization variables are studied at three levels represented in coded

TABLE 3 Test optimization variables levels of the design variable

Optimization variables	Factor level -1	0	1
H_{PM}	3.5 mm	4.0 mm	4.5 mm
τ_r	19.6 mm	21.3 mm	23.0 mm
δ	3.5 mm	4.0 mm	4.5 mm
t_s	9.0 mm	10.0 mm	11.0 mm

TABLE 4 Experimental design and results

	Factor level				Objectives		
No	τ_r	H_{PM}	g	t_s	P (W)	F (N)	η (%)
1	-1	-1	-1	-1	1164.68	406.23	90.94
2	1	-1	-1	-1	1278.64	783.56	90.95
3	-1	1	-1	-1	1380.75	814.09	90.95
4	1	1	-1	-1	1485.29	1428.56	90.96
5	-1	-1	1	-1	931.55	165.84	90.92
6	1	-1	1	-1	1042.79	374.94	90.94
7	-1	1	1	-1	1168.11	351.95	90.94
8	1	1	1	-1	1270.17	784.54	90.95
9	-1	-1	-1	1	1270.40	312.60	91.06
10	1	-1	-1	1	1435.05	493.70	91.08
11	-1	1	-1	1	1595.82	344.60	91.08
12	1	1	-1	1	1749.45	984.42	91.10
13	-1	-1	1	1	954.58	189.54	91.05
14	1	-1	1	1	1095.92	246.20	91.06
15	-1	1	1	1	1274.9	219.76	91.07
16	1	1	1	1	1422.23	524.33	91.08
17	-1	0	0	0	1240.55	221.42	91.01
18	1	0	0	0	1375.44	603.00	91.02
19	0	-1	0	0	1163.02	202.95	91.00
20	0	1	0	0	1441.71	591.54	91.03
21	0	0	-1	0	1458.64	573.68	91.02
22	0	0	1	0	1179.29	249.67	91.01
23	0	0	0	-1	1302.82	547.71	90.98
24	0	0	0	1	1365.31	252.66	91.07
25	0	0	0	0	1316.05	369.36	91.02

form by 1, 0 and 1. And the experiment consists of 25 tests are conducted for the four optimization variables according to the CCD theory. The experimental data are obtained by computer simulations in this paper. The test optimization variables levels are shown in Table 3, and the experimental design and results are shown in Table 4.

Based on the experimental results, the estimated regression coefficients are calculated and the three response surface models including the output power, the detent force, and the efficiency are obtained and shown in Equations (4)–(6):

$$P = -3182.37 + 244.02\tau_r + 539.01H_{PM} + 232.4\delta - 70.62t_s \sim + 6.44\tau_r t_s + 49.98H_{PM}t_s - 50.79\delta t_s - 6.34\tau_r^2 - 95.8H_{PM}^2 \quad (4)$$

$$F = 11265.14 - 900.8\tau_r\delta + 183.95H_{PM} - 1694.21\delta + 246.26t_s + 85.83\tau_r H_{PM} - 59.79\tau_r\delta - 16.59\tau_r t_s - 167.88H_{PM}\delta - 102.19H_{PM}t_s + 99.96\delta t_s + 25.03\tau_r^2 + 257.15\delta^2 \quad (5)$$

$$\eta = 90.28 + 4.19 \times 10^{-3}\tau_r + 0.02H_{PM} - 0.01\delta + 0.06t_s \quad (6)$$

4.2 | Multi-objective optimization

During the optimization process, the improvement of power density and the efficiency often leads to the undesirable increase of detent force. So, a tradeoff design is often required. To realize a tradeoff among the power density, the efficiency and the detent force, and obtain the optimal combination of the optimization variables accurately, the multi-objective genetic algorithm method (MOGA) is applied in this part [25]. The genetic algorithm (GA) fitness function is proposed based on the response surface analytical model equation of the optimization objectives, which can be expressed as the follow equation:

$$f(x_i) = \lambda_P \frac{P'}{P(x_i)} + \lambda_F \frac{F(x_i)}{F'} + \lambda_\eta \frac{\eta'}{\eta(x_i)} \quad (7)$$

where x_i is the main optimization variables of the 120°-TPMLG, P, F and η are the initial values of the output power, the detent force, and the efficiency, respectively, while $P(x_i)$, $F(x_i)$ and $\eta(x_i)$ are the three optimized values.

To achieve the desired performance of the three optimization objectives and obtain relatively high efficiency of the seeking optimization, some special constraints are defined as follows:

By using the MOGA, a series of feasible design points is sought out effectively, which is shown in Figure 7.

According to the objective functions and constraints in Table 5, two feasible design points are selected to be the candidate design points of the optimal 120°-TPMLG, namely candidate design 1 and candidate design 2. The corresponding values of the optimization variables and optimization objectives of the 120°-TPMLG are listed in Table 6. It can be observed from the table that the maximum output power can reach 1292.60 W in candidate design 1, which is 6.39% higher than that in candidate design 2. The minimum detent force can achieve 162.94 N in candidate design 2, which is 19.93% low than that in candidate design 1. The efficiency of the candidate design 1 and candidate design 2 are almost same, which is about 91.05%. Considering a compromise between the output power, the efficiency and the detent force, candidate design 2 is chosen to be the final optimized design for the 120°-TPMLG, where

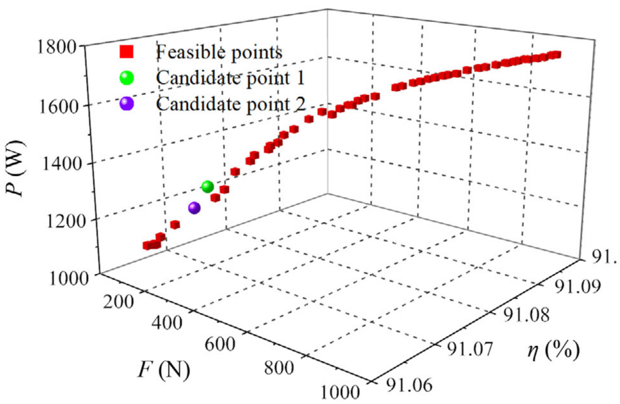

FIGURE 7 Feasible design points after optimization

TABLE 5 Special constraints of the 120°-TPMLG

Items	Constraints
P	$P > 1.2$ kW
F	$F < 200$ N
H	$\eta > 90\%$
Rate speed	0.4 m/s
Rate load	40 Ω

TABLE 6 Optimization results

Items		Candidate design	
		Candidate design 1	Candidate design 2
Optimization variables	H_{PM}	3.8 mm	3.7 mm
	τ_r	21.1 mm	21 mm
	δ	4 mm	4.1 mm
	t_s	11 mm	11 mm
Optimization objectives	P_{out}	1292.60 W	1214.86 W
	F	195.41 N	162.94 N
	η	91.05%	91.05%

τ_r, H_{PM}, g, and t_s are 21 mm, 3.7 mm, 4.1 mm and 11 mm, respectively.

5 | PERFORMANCES ANALYSIS

To verify the effectiveness of the proposed optimization method, the optimal generator model of the 120°-TPMLG (optimal generator) are constructed based on optimal structural parameters in the Table 7, and its performances are analysed and compared with those of the initial design model of the 120°-TPMLG (initial generator) by the finite element analysis software of Magnet. To ensure the accuracy of the calculation results, the time step is set to 1 ms. Besides self-adaptive mesh refine is adopted, and the maximum element size of the mesh is set to 3 mm.

TABLE 7 Comparison of value of the optimization variable

Optimization variables	Generator type	
	Initial generator	Optimal generator
H_{PM}	3.5 mm	3.7 mm
τ_r	21.3 mm	21 mm
δ	4 mm	4.1 mm
t_s	11 mm	11 mm

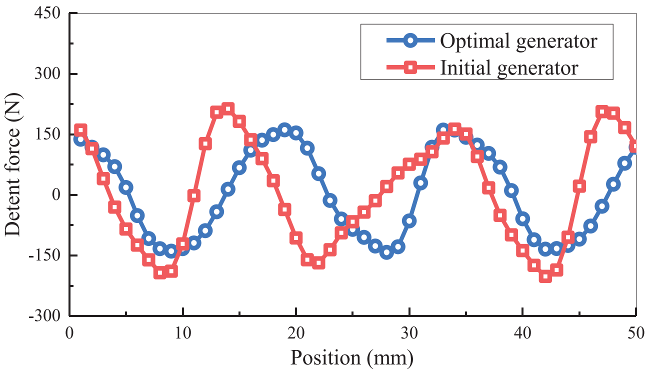

FIGURE 8 Analysis of detent force of the two generators

5.1 | Performance analysis at a constant speed

In general, the speed of the translator is assumed to be a constant value, that is, 0.4 m/s, to facilitate the analysis of the generators. The detent force, no-load EMF, voltage, output power, losses and efficiency of the two generators on the speed of 0.4 m/s are investigated and compared in this section.

The detent force of the two generators is analysed and compared in Figure 8.

As shown in Figure 8, we can find that the maximum detent force for the optimal generator is decreased to 162.94 N from 213.70 N for the initial generator, which represents 31.15% detent force is reduced through optimization.

The no-load EMF of the two generators are shown and compared in Figure 9.

As shown in Figure 9, it can be seen that the amplitude of the three phase EMF of the optimal generator are higher than that of the initial generator. The corresponding spectral analysis results are shown in Figure 10.

As shown in Figure 10, the three-phase EMF fundamental amplitudes of the optimal generator are 216.53, 195.32, and 212.85 V, which increase about 1.52%, 3.87%, and 0.11% than that of the initial generator, respectively. The total harmonic distortion of the phase B and phase C EMF is decreased by 0.07%

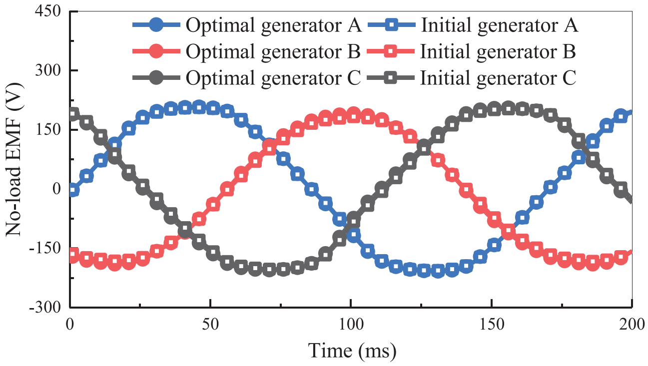

FIGURE 9 Analysis of the three-phase no-load EMF

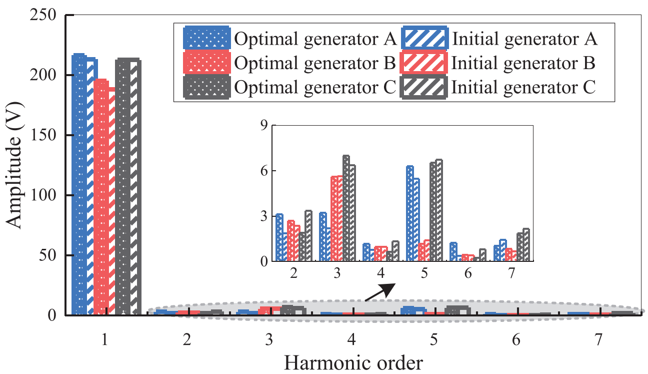

FIGURE 10 Spectral analysis of three-phase no-load EMF

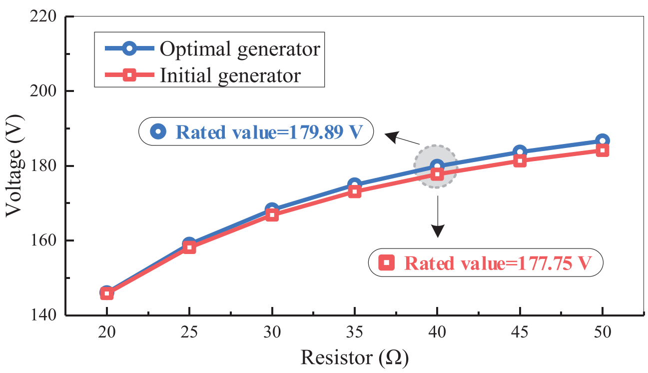

FIGURE 11 Analysis of the voltage

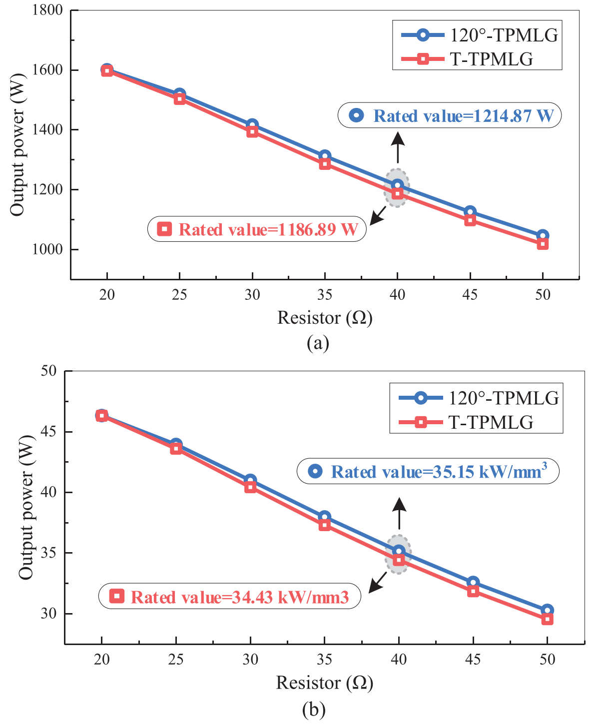

FIGURE 12 Analysis of the output power and power density. (a) Output power; (b) power density

and 0.21% than that of the initial generator. Nevertheless, the total harmonic distortion of phase C EMF of the optimal generator is undesirable increase by 0.71% than that of the initial generator.

The performances with different resistance loads are analysed and compared with that of the initial generator to investigate the load characteristics of the optimal generator. The voltage of the two generators is analysed and compared in Figure 11.

As shown in Figure 11, it can be observed that the voltage of the optimal generator is higher than that of the initial generator on the same resistor loads. When the resistance load is 40 Ω, the voltage of the optimal generator is 179.90 V, which is 1.20% higher than that of the initial generator. Therefore, the optimal generator has a higher voltage than the initial generator.

The output power and the power density of the two generators are shown and compared in Figure 12.

As shown in Figure 12, the output power and the power density of the two generators have a downward trend with the increase of the resistance loads, and the output power and the power density of the optimal generator are higher than that of the initial generator under the same resistance loads. When the resistance load is 40 Ω, the output power and power density of the optimal generator is 1214.87 W and 35.15 kW/m^3, which is 2.53% and 2.09% higher than that of the initial generator, respectively. Therefore, the performance of the optimal generator is better than that of the initial generator in terms of the output power and the power density.

Ignoring the mechanical loss and stray loss, the generator losses usually include the iron loss and copper loss of the armature windings, which have a large effect on generation efficiency of the generator. The generation efficiency can be calculated as:

$$\eta = \frac{P_{out}}{P_{out} + P_{Cu} + P_{Fe}} \tag{8}$$

where η is the generation efficiency, P_{out} is the output power, P_{Cu} is the copper loss and P_{Fe} is the iron loss;

The performances of losses and efficiency of the two generators under different loads are shown in Figure 13.

As shown in Figure 13, when the resistance loads increased, the losses of the two generators decreased, the generation

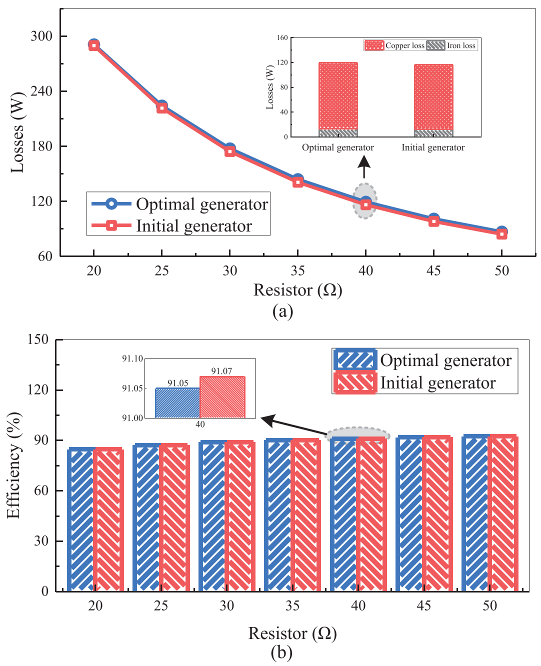

FIGURE 13 Analysis of losses and efficiency. (a) Losses; (b) efficiency

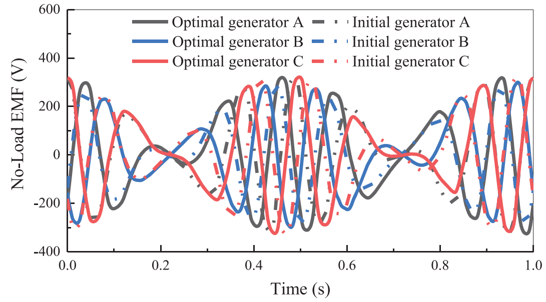

FIGURE 14 Analysis of No-load EMF at the sinusoidal speed

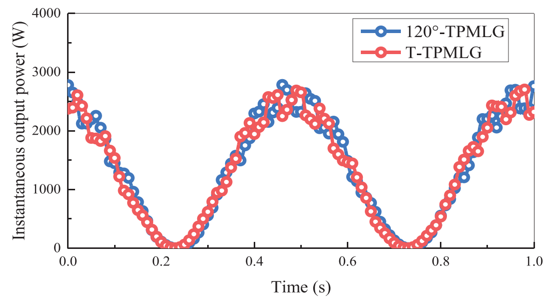

FIGURE 15 Analysis of output power at the sinusoidal speed

efficiency increased. When the resistance load is 40 Ω, the total losses of the optimal generator is 2.67% higher than that of the initial generator. Nevertheless, the efficiency of the optimal generator is only 0.02% lower than that of the initial generator due to that the output power of the optimal generator is higher 2.57% than that of the initial generator, which means that the efficiency of the generators is almost the same before and after optimization.

According to the analysis above, it can be observed that, through optimization, the performances of the 120°-TPMLG have a notably improvement in term of detent force, which is decreased by 31.15%. Besides, the other performance including output power, and power density also have a slight improvement, in which the output power is increased by 2.53% and the power density is increased by 2.09%.

5.2 | Performance analysis at a sinusoidal speed

The above analysis is conducted at the constant speed of 0.4 m/s for the purpose of simplicity. Nevertheless, on the real oceanic condition, the speed of waves is approximate sinusoidal speed, which is relative to the wave height H and angular frequency ω [26]. According to the condition of the Yellow Sea, where the wave height $A = 0.2$ mm and the wave period $T = 2$ s, the speed of the 120°-TPMLG can be expressed as:

$$v(t) = 0.628 \cos(6.28t) \tag{9}$$

The no-load EMF of the two generators on the sinusoidal speed of $v(t) = 0.628\cos(6.28t)$ is analysed and compared in Figure 14.

According to the Figure 14, it can be seen that the three-phase no-load EMF peak value of the optimal generator are 319.45 V, 299.82 V and 321.57 V, which is 0.87%, 5.37% and 1.03% higher than that of the initial generator, respectively. Consequently, the optimal generator has a higher three-phase no-load EMF than the initial generator at the sinusoidal speed.

The output power of the two generators at the sinusoidal speed is analysed and compared in Figure 15.

As shown in Figure 15, the instantaneous output power of the optimal generator is higher than that of the initial generator. And the average power and the maximum instantaneous power of the optimal generator is 1402.84 and 2782.22 W, which are 1.87% and 1.41% higher than that of the initial generator, respectively. Therefore, the optimal generator has a higher output power than the initial generator at the sinusoidal speed.

According to the analysis above, it can be observed that the performance of the 120°-TPMLG is slightly improved in term of output power at the sinusoidal speed after optimization, in which the average power and the maximum instantaneous power are increased by 1.87% and 1.41%, respectively.

5.3 | FEA credibility and 120°-TWs reasonableness validation

The proposed 120°-TPMLG can be converted from the PMRG, where the main dimensions of the 120°-TPMLG is confirmed by utilizing the measurement relationship between the PMRG and TPMLG [19]. Therefore, to verify the credible of the above finite element analysis method and the reasonable of the proposed winding configuration (120°-TWs), a PMRG prototype

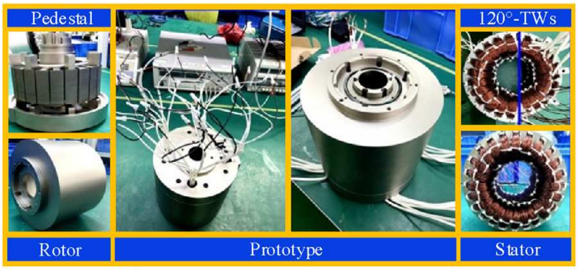

FIGURE 16 Prototype of the 120°-PMRG

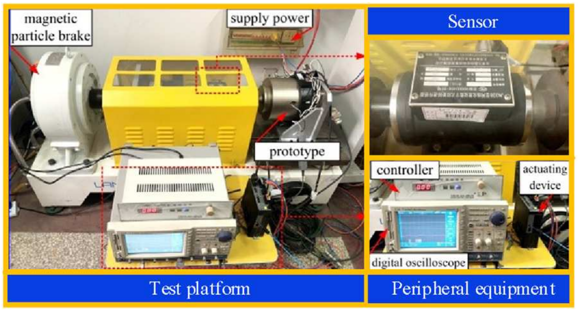

FIGURE 17 Test platform

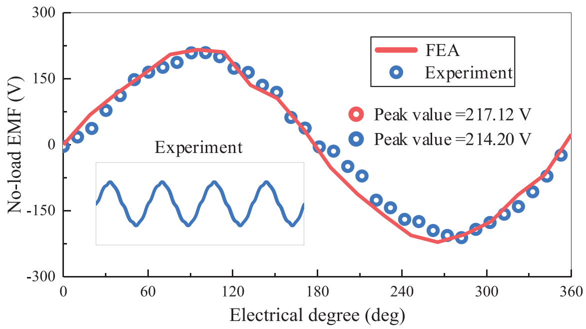

FIGURE 18 Comparison of the no-load EMF of the FEA and the experiment at constant velocities

with the same 120°-TWs (120°-PMRG) can be used in the experiment. Figure 16 shows the prototype of the 120°-PMRG, which includes the pedestal, rotor, stator yoke and 120°-TWs. The corresponding test platform for the generator is shown in Figure 17.

When the120°-PMRG runs at a constant velocity, its no-load EMF can be obtained as shown in Figures 18 and 19. Figure 18 shows the comparison of the no-load EMF waveform of the FEA and the experiment at the constant linear velocity of 1k rpm. Figure 19 shows the comparison of the no-load EMF of the FEA and the experiment at different constant velocities.

It can be seen from Figures 18 and 19 that the EMF obtained by FEA agrees with the experimental ones, which demonstrate the FEA method used to analyze the performance is accurate and the 120°-TWs is reasonable. Therefore, the analysis results obtained by the same analysis method (FEA) are credible in this paper.

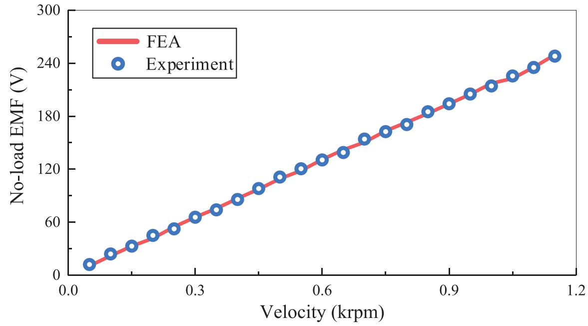

FIGURE 19 Comparison of the no-load EMF of the FEA and the experiment at different velocities

6 | CONCLUSION

In this paper, a new multi-objective optimization method is proposed for the 120°-TPMLG, where the RS method and the genetic algorithm are co-applied to realize the fast search of the best structural parameter combination. To verify effectiveness of the proposed multi-objective optimization method, the performances of the optimal generator is analysed and compared with that of the initial generator. It is demonstrated by the comparison results that the power density is increased by 2.09%, the detent force is desirably decreased 31.15%, and the efficiency of are almost constant under rated condition ($v = 0.4$ m/s, $R = 40$ Ω). Therefore, the proposed optimization method is effective for the 120°-TPMLG.

ACKNOWLEDGEMENTS

The authors would like to thank Shu-hua Wang and the Yokokawa Robot (Shenzhen) Co., Ltd for technical support.

FUNDING

This work is partially supported Natural Science Foundation of China under grant No.51777060, in part by the Major Special Project for Collaborative Innovation in Zhengzhou No. 20XTZX12023. and the China Postdoctoral Science Foundation (2020M682342).

CONFLICT OF INTEREST

Authors have no conflict of interest to declare.

DATA AVAILABILITY STATEMENT

Research data are not shared.

ORCID

Jikai Si https://orcid.org/0000-0002-9663-2349
Yihua Hu https://orcid.org/0000-0002-1007-1617

REFERENCES

1. Yuping, G., Shuangquan, S., Huiming, Z., et al.: A fully floating system for a wave energy converter with direct-driven linear generator. Energy 95, 99–109 (2016). https://www.webofscience.com/wos/alldb/full-record/WOS:000370308100010
2. Chen, H., Zhang, Y., Wang, H., et al.: A tubular permanent magnet linear generator with novel structure. IEEE Trans. Plasma Sci.

47(6), 2995–3001 (2019). http://www.webofscience.com.zzulib.vpn358.com/wos/woscc/full-record/WOS:000470969700028?UT=WOS:000470969700028&SID=6EADN8Ko9ikqhPWr1or
3. Elwood, D., Yim, S.C., Prudell, J., et al.: Design, construction, and ocean testing of a taut-moored dual-body wave energy converter with a linear generator power take-off. Renewable Energy 35(2), 348–354 (2010). https://www.webofscience.com/wos/alldb/full-record/WOS:000271688300005
4. Trapanese, M., Boscaino, V., Cipriani, G., et al.: A permanent magnet linear generator for the enhancement of the reliability of a wave energy conversion system. IEEE Trans. Ind. Electron. 66(6), 4934–4944 (2019). https://www.webofscience.com/wos/alldb/summary/f16c1b50-d319-4f0e-aa49-726da9968e12-128d4827/relevance/1
5. Si, J., Yan, Z., Xu, S.: Optimal design of a tubular permanent magnet linear generator with 120°phase belt toroidal windings for detent force reduction. Trans. China Electrotech. Soc. 36(6), 1138–1148 (2021). https://www.webofscience.com/wos/alldb/summary/484961ab-0477-4ab3-bf7d-19eba5bf5e2c-128d90a9/relevance/1
6. Guo, Y., Si, J., Gao, C., et al.: Improved fuzzy-based taguchi method for multi-objective optimization of direct-drive permanent magnet synchronous motors. IEEE Trans. Magn. 55(6), 1–4 (2019). https://www.webofscience.com/wos/alldb/summary/fc979a18-7330-4022-afff-5f15913fcd89-128db600/relevance/1
7. Si, J., Zhao, S., Feng, H., et al.: Multi-objective optimization of surface-mounted and interior permanent magnet synchronous motor based on Taguchi method and response surface method. Chinese J. Electr. Eng. 4(1), 67–73 (2018). https://www.webofscience.com/wos/alldb/full-record/INSPEC:17750469
8. Xu, L., Zhao, W., Liu, G., et al.: Design optimization of a spoke-type permanent-magnet Vernier machine for torque density and power factor improvement. IEEE Trans. Veh. Technol. 68(4), 3446–3456 (2019). https://www.webofscience.com/wos/alldb/full-record/WOS:000465241600033
9. Liu, G., Wang, Y., Chen, Q., et al.: Multi-objective Optimization of an Asymmetric V-Shaped Interior Permanent Magnet Synchronous Motor. Transactions of China Electrotechnical Society 32(2), 385–393 (2019). https://d.wanfangdata.com.cn/periodical/ChlQZXJpb2RpY2FsQ0hJTmV3UzIwMjExMDI2Eg9kZ2pzeGIyMDE4ejIwMTcaCDM5czY3aHA5
10. Zhu, X., Jiang, M., Xiang, Z., et al.: Design and optimization of a flux-modulated permanent magnet motor based on an air gap-harmonic-orientated design methodology. IEEE Trans. Ind. Electron. 67(7), 5337–5348 (2020). https://www.webofscience.com/wos/alldb/full-record/WOS:000521375400011
11. Asef, P., Perpiñá, R.B., Barzegaran, M.R., et al.: Multi-objective design optimization using dual-level response surface methodology and Booth's algorithm for permanent magnet synchronous generators. IEEE Trans. Energy Convers. 32(2), 652–659 (2017). https://fx.zzu.superlib.net/detail_38502727e7500f26bddb42afdb7e221d8a0774a8f6f95c0f1921b0a3ea255101e580949000984f4b09b78c71ea9c226359a2e1c5afdb9d18c45348fd09ef338716eceeed8eb6373848542f77906a08e5?
12. Xu, W., Wang, X., Junejo, A.K., et al.: Analysis and Optimization of Torque Ripple Reduction Strategy of Surface-Mounted Permanent-Magnet Motors in Flux-Weakening Region Based on Genetic Algorithm. IEEE Trans. Ind. Appl. 57(4), 4091–4106 (2021). https://www.webofscience.com/wos/alldb/full-record/WOS:000673633200077
13. Guo, Z., Liang, Y., Bian, X., et al.: Multi-objective optimization for arrangement of the asymmetric-paths winding based on improved discrete particle swarm approach. IEEE Trans. Energy Convers. 13(3), 1571–1578 (2018). https://www.webofscience.com/wos/alldb/full-record/WOS:000443085800063
14. Lei, G., Xu, W., et al.: Multilevel design optimization of a FSPMM drive system by using sequential subspace optimization method. IEEE Trans. Magn. 50(2), 7016904 (2014). Jiefeng. https://www.webofscience.com/wos/alldb/full-record/WOS:000332471700168
15. Gao, J., Dai, L., Zhang, W., et al.: Improved genetic optimization algorithm with subdomain model for multi-objective optimal design of SPMSM. CES Trans. Electrical Mach. Syst. 2(1), 160–165 (2018). https://www.webofscience.com/wos/alldb/full-record/INSPEC:17736377
16. Lee, J.H., Kim, J.-W., Song, J.-Y., et al.: Distance-based intelligent particle swarm optimization for optimal design of permanent magnet synchronous machine. IEEE Trans. Magn. 53(6), 7206804 (2017). https://www.webofscience.com/wos/alldb/full-record/WOS:000403480400104
17. Xiang, Z., Zhu, X., Li, Q., et al.: Multilevel design optimization and operation of a brushless double mechanical port flux-switching permanent-magnet motor. IEEE Trans. Ind. Electron. 63(10), 6042–6054 (2016). https://www.webofscience.com/wos/alldb/full-record/WOS:000384641900007
18. Si, J., Zhang, L., Feng, H., et al.: Multi-objective optimal design of a surface-mounted and interior permanent magnet synchronous motor. J. China Coal Soc. 41(12), 3167–3173 (2016). https://www.webofscience.com/wos/alldb/full-record/CSCD:5894713
19. Si, J., Feng, H., Su, P., et al.: Design and analysis of tubular permanent magnet linear wave generator. Sci. World J. 65(9), 1–7 (2014). https://www.researchgate.net/publication/264127390_Design_and_Analysis_of_Tubular_Permanent_Magnet_Linear_Wave_Generator
20. Saltelli, A., et al.: Sensitivity Analysis in Pratice: A Guide to Assessing Scientific Models. John Wiley and Sons, Chichester (2008). https://www.wiley.com/en-us/Sensitivity+Analysis+in+Practice%3A+A+Guide+to+Assessing+Scientific+Models-p-9780470870945
21. Moghaddam, I.N., Salami, Z., Easter, L., et al.: Sensitivity Analysis in an Excitation System in order to simplify and validate dynamic model utilizing plant test data. IEEE Trans. Ind. Appl. 51(4), 3435–3441 (2015). https://www.webofscience.com/wos/alldb/full-record/WOS:000358255700075
22. Wen, C., Yu, H., Hong, T., et al.: Coil shape optimization for superconducting wind turbine generator using response surface methodology and particle swarm optimization. IEEE Trans. Appl. Supercond. 24(3), 5202404 (2014). https://www.webofscience.com/wos/alldb/full-record/WOS:000348398400001
23. Shangguan, X., Sun, Z., Wang, Q., et al.: Electromagnetic torque optimization in multi-segment and double-layer interior permanent magnet machine. Small Special Electr. Mach. 45(5), 8–14 (2017). http://en.cnki.com.cn/Article_en/CJFDTotal-WTDJ201705003.htm
24. Liu, X., Fu, W.N.: A dynamic dual-response-surface methodology for optimal design of a permanent-magnet motor using finite-element method. IEEE Trans. Magn. 50(3), 7204304 (2016). https://www.webofscience.com/wos/alldb/full-record/WOS:000372254000100
25. Lei, G., Wang, T., Zhu, J., et al.: System-level design optimization methods for electrical drive systems-robust approach. IEEE Trans. Ind. Electron. 62(8), 4702–4713 (2015). https://www.webofscience.com/wos/alldb/full-record/WOS:000357268300005
26. Prudell, J., Stoddard, M., Amon, E.: Annette von Jouanne: A permanent-magnet tubular linear generator for ocean wave energy conversion. IEEE Trans. Ind. Appl. 46(6), 2392–2400 (2010). https://xueshu.baidu.com/usercenter/paper/show?paperid=0e9a87e9cb82afa267b2fa17ffac27b6

SUPPORTING INFORMATION

Additional supporting information may be found in the online version of the article at the publisher's website.

How to cite this article: Si, J., Yan, Z., Nie, R., Li, Z., Hu, Y., Li, Y., et al.: Multi-objective optimization of a tubular permanent magnet linear generator with 120° phase belt toroidal windings using response surface method and genetic algorithm. IET Renew. Power Gener. 16, 352–361 (2022). https://doi.org/10.1049/rpg2.12328